Nat Methods. Author manuscript; available in PMC 2016 October 12.

Published in final edited form as:

Nat Methods. 2013 December ; 10(12): 1225–1231. doi:10.1038/nmeth.2684.

High-throughput fingerprinting of human pluripotent stem cell factor responsiveness and lineage induction bias

Emanuel J.P. Nazareth[1], **Joel E.E. Ostblom**[2], **Petra B. Lücker**[1,3], **Shreya Shukla**[1], **Manuel M. Alvarez**[1], **Steve K.W. Oh**[4], **Ting Yin**[1], and **Peter W. Zandstra**[1,3,5,6]

[1]Institute of Biomaterials and Biomedical Engineering, University of Toronto, Toronto, Ontario, Canada

[2]Department of Medical Biochemistry and Biophysics, Karolinska Institutet, Stockholm, Sweden

[3]Department of Chemical Engineering and Applied Chemistry, University of Toronto, Toronto, Ontario, Canada

[4]Bioprocessing Technology Institute, A*STAR (Agency for Science, Technology and Research), Singapore, Singapore

[5]McEwen Centre for Regenerative Medicine, University Health Network, Toronto, Ontario, Canada

[6]Heart and Stroke Richard Lewar Centre of Excellence, Toronto, Ontario, Canada

Abstract

Populations of cells create local environments that lead to emergent heterogeneity. This is particularly evident in human pluripotent stem cells (hPSCs) where microenvironmental heterogeneity limits cell fate control. We have developed a high-throughput platform to screen hPSCs in configurable micro-environments, enabling the optimization of colony size, cell density, and additional parameters for rapid and robust cell fate responses. Single-cell protein expression profiling revealed that Oct4 and Sox2 co-staining discriminate pluripotent, neuroectoderm, primitive streak, and extraembryonic cell fates, allowing dose responses of 27 developmental factors to simultaneously delineate lineage-specific concentration optima. This platform also enabled quantification of endogenous signaling pathway activation and differentiation bias (fingerprinting). Short-term (48 h) fingerprinting is predictive of definitive endoderm induction efficiency across 12 cell lines and was used *a priori* to rescue long-term (>18 day) differentiation of a cell line reticent to cardiac induction. These findings facilitate high-throughput hPSC-based screening and quantification of lineage induction bias.

Correspondence should be addressed to: P.W.Z. (peter.zandstra@utoronto.ca).

Competing Financial Interests

The authors declare no competing financial interests.

Author Contributions

E.J.P.N. designed, performed and analyzed most experiments. J.E.E.O. assisted with immunocytochemistry and software development. P.L. performed cardiac induction experiments. S.S. created hiPSC lines. T.Y. performed endoderm induction experiments. M.A. and T.Y. provided cell culture support. S.K.W.O. provided editorial input on the manuscript. E.J.P.N. and P.W.Z. designed the project and wrote the manuscript.

Introduction

Human pluripotent stem cells (hPSCs) offer opportunities for drug development, understanding mechanisms of human cell development and cell-based therapies, but this requires a predictive understanding of cell fate controlling factors. Although much progress has been made in this effort, confounding factors frequently limit reproducibility and biological insight. For example, fibroblast growth factor (FGF)[1, 2], activin A[3, 4], leukemia inhibitory factor (LIF)[5, 6] and Wnt[7, 8] signaling have been reported to both maintain pluripotency of hPSCs and have no effect on maintenance. The International Stem Cell Initiative (ISCI) recently reported the first multi-laboratory comparative study of published defined culture systems for hPSC expansion[9]. Surprisingly, only two out of eight media tested reproducibly maintained hPSCs across laboratories and cell lines, highlighting the need to identify and control key confounding factors.

Population context can have dramatic consequences on stem cell maintenance, differentiation and reprogramming. HPSCs exist in complex microenvironments containing multiple factors that regulate cell fate, including endogenous ligands and extra-cellular matrix proteins[10], mechanical forces and cell-cell contact[11], and cell subpopulations[2, 10]. Critically, these factors are spatially heterogeneous between cells[10], introducing substantial variances in cell response. Indeed, reprogramming to pluripotency [12], differentiation towards neural[13], pancreatic[14] and cardiac[15] cell types, and the disease phenotype of a familial dilated cardiomyopathy (DCM) induced hPSC model[16] all have specific organizational and density dependent optima.

We have developed a suite of tools to study hPSCs, including a novel method of patterning cells in 96-well plates, an optimized assay protocol, defined media and substrate, and a single-cell imaging and data analysis pipeline. Applying this platform revealed that colony size, cell density, media composition and substrate are major determinants of cell response to exogenously applied factors and that optimization of these parameters allows rapid and robust cell fate responses to be measured in 48h. Characterization of single cell protein expression across diverse induction conditions revealed that Oct4 and Sox2 costaining can discriminate pluripotent, neuroectoderm, primitive-streak, and extraembryonic subpopulations, allowing simultaneous tracking of these subpopulations. Application of this platform to characterize 27 developmental signaling factors selected by the ISCI consortium across a wide range of doses revealed new dose- and lineage-specific optima. For example, dose response analysis of LDN-193189[17] revealed an optimal pluripotency response at 2.5 μM and optimal neuroectoderm induction at 10 μM, underscoring the utility of simultaneous subpopulation tracking. The platform also enabled quantitative comparisons of cell line response to diverse lineage induction stimuli (fingerprinting). These responses were found to be stable between passages, variable between cell lines, predictive of lineage induction efficiency (as we show for both definitive endoderm and cardiac induction), and can be used to improve differentiation of reticent cell lines. These findings provide a method to rapidly test hPSC responses to exogenous factors and to categorize cell lines based on differentiation bias.

Results

Controlling the microenvironment for rapid hPSC screening

We previously developed an assay in which hPSC distribution (colony size, shape, and spacing) can be controlled by micro-contact printing (μCP) substrates onto slides. This work indicated that colony size control could be a powerful tool in stem cell screens[10]. To adapt this technique for high-throughput (HTP) studies, we developed a novel method of μCP in which substrates are directly printed into 96-well plates in user-defined patterns (Supplementary Fig. 1) and a fully defined and disclosed serum-free media (SF) and substrate (a fibronectin and gelatin mixture, "FnGel") (Supplementary Fig. 2). The 96-well assay consists of dispensing a single cell suspension into the wells, allowing the cells to settle and adhere to the patterned substrate for 6 h, washing away non-adherent cells, adding test factors to the wells for 42 h, and then fixing and analyzing the plates (Fig. 1a). Each well contains an array of hPSC colonies, and automated microscopy was used to obtain single cell data such as x- and y-coordinates and expression levels of proteins (Fig. 1b).

Based on our current mechanistic understanding of the relation between colony size and endogenous signaling[10], we reasoned that calibration of colony size would allow robust detection of both positive and negative regulators of pluripotency and differentiation bias. To test this, we assayed the response of hPSCs (H9 line) to different colony sizes under various conditions including murine embryonic fibroblast conditioned media (CM), SF base media alone, and SF with fibroblast growth factor 2 (FGF2) and the transforming growth factor beta (TGFβ) inhibitor SB431542 (FTi), SF with bone morphogenetic protein 4 (BMP4, B), or SF with BMP4 with and activin A (BA) (Fig. 1c). Frequencies of cells expressing the pluripotency factors Oct4 and Sox2 were colony-size dependent, with cells in SF alone maintaining high pluripotency in 1200 μm colonies and dramatically losing pluripotency in 150 μm colonies. Relative to baseline SF conditions, hPSCs in 200 μm colonies were found to respond to CM (ANOVA, $p = 1.17\times10^{-5}$) and B (ANOVA, $p = 2.74\times10^{-4}$), indicating that this colony size was ideal for our test criteria. Based on the above results and additional optimization of parameters such as cell density (see Supplementary Results, Supplementary Fig. 3–5), a final assay configuration (the "96μCP" platform) was determined for all subsequent 96-well assays (Supplementary Table 1). These results demonstrate that stem cell microenvironment parameters can be engineered to enable fully defined HTP screens with more robust responses and faster kinetics.

Oct4 and Sox2 expression discriminate early cell fates

We next sought to determine if early lineage specification, in addition to pluripotency, could be quantified using the 96μCP platform. We chose six previously characterized conditions: CM (maintains pluripotency[18]), heregulin-1β with activin A and FGF2 ("HAF") (maintains pluripotency[19]), B (induces trophectoderm and primitive endoderm[20–22]), BA (induces primitive streak[22]) and FTi (induces neuroectoderm[23, 24]). For all conditions, we assessed single-cell protein expression of a panel of early developmental lineage markers including pluripotency (Oct4, Sox2, Nanog, Tra-1-60), primitive streak (Brachyury, Gata4, Snail), neural (Pax6, Sox1, Sox3), extraembryonic (Sox7, CDX2, Hand1), endoderm (CXCR4, Foxa2) and mesoderm markers (Brachyury, Gata4) (select images shown in Fig. 2a). Several

later stage markers, typically arising more than 6 days post-induction, including Pax6, Sox1, Sox3, Sox7, CDX2, Hand1, and CXCR4, showed no difference in expression, indicating that at this very early test point (42 h) these markers are not differentially expressed, as expected.

Two dimensional hierarchical clustering, performed on the protein expression results across the control conditions (Fig. 2b) confirmed that different induction conditions result in distinct protein expression profiles. Note that thresholds for positive expression were determined for each protein based on differential expression across control conditions (Fig. 2c). SF and FTi conditions clustered together, indicating that under basal conditions the hPSCs are largely neuroectoderm fated, in line with previous observations indicating a "default" neuroectoderm fate in the absence of primitive streak inducing factors[25]. $Oct4^{-}Sox2^{+}$, previously shown to mark committed neural precursors in human[26] and mouse[27] development, was found to be expressed exclusively in the neuroectoderm-inducing conditions FTi and SF. $Oct4^{-}Sox2^{-}$ expression clustered separately from the other groups, interpreted as marking a non-pluripotent, non-neural, non-primitive streak population, likely fated towards extraembryonic tissue (trophectoderm and primitive endoderm). Primitive streak markers also clustered together, and intriguingly $Oct4^{+}Sox2^{-}$ expression also clustered with this group. To verify that $Oct4^{+}Sox2^{-}$ could be used as a surrogate for early primitive streak induction, we confirmed that across all control conditions $Oct4^{+}Sox2^{-}$ is exclusively found in the BA condition, which induces primitive streak (Fig. 2d and Fig. 2e), and is exclusively associated with high expression levels of Snail, Brachyury, and Gata4 (Fig. 2f).

This data supports the use of Oct4 and Sox2 as a binary code to discriminate four major early cell fates in human development: $Oct4^{+}Sox2^{+}$ for pluripotency, $Oct4^{-}Sox2^{+}$ for early neuroectoderm, $Oct4^{+}Sox2^{-}$ for early primitive streak, and $Oct4^{-}Sox2^{-}$ for early extraembryonic committed and other tissues (Fig. 2g). This classification is congruent with previous reports of Oct4 and Sox2 expression in these lineages[20, 28–30]. Although additional markers will increase fate, this simple code represents a minimal set suitable for simultaneous early lineage screening, as shown below.

High content analysis of early hPSC cell fate responses

Using the 96μCP platform we simultaneously characterized the above four early cell fates in response to 27 developmental factors. Responding factors (Fig. 3a, non-responding factors in Supplementary Fig. 6) were classified as generally promoting pluripotency, neuroectoderm, primitive streak, extraembryonic/other, or having a bimodal effect (inducing different subpopulations at different concentrations). We have summarized the classification of these factors as well as a recommended concentration for use in chemically defined media in Table 1.

Several factors resulted in profiles predicted from literature. FGF2[3], TGFβ1 and a ctivin A[31], heregulin-β1[19], IGF1[19], and noggin[32] all increased pluripotency. Previously, a 7 day non-patterned hPSC-based screen of 806 human extracellular factors assaying for pluripotency regulators found that only FGF2 and pigment epithelium-derived factor substantially increased pluripotency in hPSCs, with TGFβ1, activin A, heregulin- β1, IGF-1, noggin, and all other factors tested having no effect[33], highlighting the improved false-

negative rate afforded by microenvironmental optimization. Also in agreement with previous observations, the TGFβ inhibitor SB431542[3](ref. 3) and the MEK inhibitor PD0325901[34](ref. 34) reduced pluripotency and increased neuroectoderm, while BMP4 suppressed pluripotency and neuroectoderm[20]. Activin A plus 40 ng mL^{-1} BMP4 resulted in a dose dependent increase in primitive streak, in contrast to activin A alone, which yielded no primitive streak[35]. LDN, an inhibitor of BMP receptors Alk2/3/6 previously uncharacterized in hPSCs, increased neuroectoderm. To determine an optimal dose to inhibit BMP signaling, we performed the LDN dose curve in the presence of BMP4 (Fig. 3b). LDN increased neuroectoderm both with and without BMP4 in a dose dependent manner up to 10 μM. Interestingly, LDN rescued pluripotency from BMP up to 2.5 μM, however at higher concentrations pluripotency decreased. Nostro et. al have shown that during endoderm induction from hPSCs there is a cell-line specific need to inhibit BMP signaling[36]. To validate LDN's ability to efficiently inhibit BMP during pancreatic progenitor induction we added 2.5 μM LDN during stage 2 of the Nostro et. al protocol, and we confirmed a significant induction of $PDX1^+$ pancreatic progenitor cells ($p = 0.0006$) (Fig. 3c). These results indicate that findings from the HTP assay are congruent with results from traditional assays and can yield predicative signaling insights applicable even to later stages of differentiation.

It has previously been reported that DKK1 has little or no effect on hPSC pluripotency. However, these studies were performed on hPSCs cultured on fibroblast feeders, measuring alkaline-phosphatase colony formation after 26 days[8]. In our assay, DKK1 had a surprising effect of inhibiting pluripotency and enhancing neuroectoderm. We speculate that endogenous supporting factors produced by the feeders mask this effect of DKK1. Indeed, when we tested the response of H9-hPSCs to DKK1 in the presence of additional factors (FGF, activin A or BMP), we found that DKK1 no longer induces neuroectoderm (Fig. 3d). This highlights the importance of characterizing endogenous background levels in interpreting cell fate decisions.

Quantification of cell-line differentiation propensities

It has long been observed that hPSCs have varying differentiation propensities[37]. We tested whether the 96μCP platform would allow a rapid evaluation of cell line specific differentiation tendencies by measuring fate responses to control conditions for 21 cell samples. Our test panel consisted of 15 hESC and hiPSC lines, including two in-house generated human induced pluripotent stem cell (hiPSC) lines, ZAN3i-85UCBT ("ZAN3") and ZAN11i-85UCBT ("ZAN11") (characterization in Supplementary Fig. 7 and Methods), an in-house generated karyotypically abnormal H7s ("H7*") with trisomy 12, which is recurrent in hPSC cultures, differentiated H9s ("H9diff") as a control, and multiple passages of H9 and ZAN11. We performed two dimensional hierarchical clustering on this data set (6 controls × 4 subpopulation measurements = 24 data points for each cell line), which enabled visualization of cell-line similarities (Fig. 4a). The H7* line expressed all pluripotency markers and had normal hPSC morphology. It was also the only line that failed to differentiate in response to BMP4, indicative of an acquired abnormality that was rapidly detected in our assay (Fig. 4b and Supplementary Fig. 8). Additionally, the three passages of

H9s and ZAN11s clustered closely, indicating that the response profile is stable over multiple passages and that the assay is highly reproducible.

As cell lines often need comprehensive cell-line-specific optimization of differentiation protocols, we sought to determine if our 2-day factor response profiles could be used to improve differentiation conditions. Despite the overall similar differentiation profile of ZAN3 and ZAN11 lines (cluster 5, Fig. 4a) and similar primitive streak induction frequency in response to BMP and activin A, we observed that when activin A is removed ZAN3s increased primitive streak induction, in contrast to ZAN11s and H9s, which decreased primitive streak induction. This trend was confirmed over multiple passages (ANOVA, $p = 0.0045$) (Fig. 4c i). To further support the primitive streak commitment of these lineages and to associate this early cell fate with functional commitment, we compared cardiac differentiation efficiency of ZAN11 and ZAN3 in an 18 day protocol[38]. We varied activin A concentration during the first four days, as differentiation is known to be sensitive to activin A in a cell-line dependent manner during this period[39]. As predicted by the day 2 results (Fig. 4c i), day 18 cardiac Troponin T (TnT) expression varied with activin A ($p = 0.0045$, Two-Factor ANOVA with $n = 2$, independent passages), with additional activin A increasing cardiomyocyte (TnT^+) output in ZAN11 but decreasing cardiomyocyte output in ZAN3 (both >95 % confidence using linear regression) (Fig. 4c ii). To further examine how correlative the day 2 96μCP response profiles are of longer periods of differentiation, we differentiated a panel of 12 hESC and hiPSC lines towards $Foxa2^+Sox17^+$ definitive endoderm using a 5 day induction protocol (Fig. 4d i and Supplementary Fig. 9a). Using the ratio of %Primitive streak induced in the BA control to %Extraembryonic in the CM condition (“Mesendoderm prediction index”), we found a significant correlation between this day 2 prediction index and cell line definitive endoderm induction efficiency at day 5 (correlation coefficient (r) = 0.89, $p = 0.0001$), demonstrating that the day two 96μCP results are indicative of longer-term differentiation (Fig. 4d ii and Supplementary Fig. 9a–b). In contrast, pluripotency of the input cell population was not correlated with definitive endoderm induction ($r = 0.29$, $p = 0.42$) (Supplementary Fig. 9c). These results demonstrate the application of our method to extract long-term cell line response from short-term response analyses.

Quantification of cell line endogenous signaling

Our results thus far and several recent studies indicate that endogenous signaling is one major source of cell line differentiation response variability. Cell line and passage-specific changes in endogenous activin A[39] and Wnt[25] signaling are known to dramatically reduce cardiac induction efficiency. By measuring responses to saturating agonists and antagonists of specific pathways, we reasoned that endogenous signaling levels could be assessed and quantitatively placed along the spectrum of low activation (endogenous response equivalent to pathway inhibitors) or high activation (endogenous response equivalent to saturating agonists). Factors that affect early cell fate decisions and saturating concentrations of these factors were determined from dose curves (Fig. 3a). Using H9s, we tested the response to agonists and antagonists of major pathways regulating hPSC fate (Fig. 4e i). To obtain an estimate of endogenous pathway activation relative to the dynamic range (“%Dynamic Range”), we combined agonist, antagonist, and base line control measurements (Eqn. 1,

Methods). The resulting endogenous signaling profile of activin, FGF, EGF, Wnt, and BMP activation in H9s is shown in Fig. 4e ii. Similar quantitative profiles were also used to compare H9s to ZAN11 and ZAN3 lines, revealing that EGF, FGF, and activin are all differentially endogenously activated (Fig. 4e iii and Supplementary Fig. 10). Comparisons of control and pathway agonist-antagonist response profiles over multiple passages indicate high correlation between passages (ZAN11 $r = 0.90$ and, ZAN3 $r = 0.88$), and lower correlation between cell lines (ZAN11 vs. ZAN3 $r = 0.52$) (Fig. 4e iv). In summary, these results show that cell lines differ in their response to induction conditions and specific pathway agonists and antagonists, and this response is stable between passages. These response profile measurements offer a novel quantitative tool for rapidly fingerprinting differentiation propensities of hPSCs.

Discussion

Heterogeneity in cell response in clonal populations arises from many cell-autonomous and non-cell-autonomous factors. Our previous work[10] and diverse evidence on hPSC culture, differentiation, and reprogramming led us to hypothesize that controlling key sources of microenvironment variance and optimizing colony size and density for robust cell response would overcome existing limitations in hPSC HTP assays. In comparison to previous HTP hPSC assays, our fully defined 96μCP platform eliminated the need to seed in CM, resulted in less variance and faster kinetics, and allowed the robust investigation of early specification of multiple lineages. Using the optimized 96μCP platform in conjunction with Oct4 and Sox2 reporting endpoint analysis allowed the screening of 27 developmental factors, providing the most comprehensive characterization of hPSC cell fate decisions to date.

Our 2 day HTP cell line response signature approach is a direct measurement of cell line response to diverse exogenous cues. Combining this phenotypically rich data set with available cell line epigenetic data and gene expression data obtained after differentiation offers an opportunity to decipher the genetic and epigenetic basis of cell-line specific responses to cues. Additionally, hiPSC cell lines can now be generated at a higher rate than they can be characterized. We propose the 96μCP platform as an effective first pass assay to detect tumorigenic cell lines and quantify neuroectoderm and primitive streak differentiation propensity. Further development may lead to a simple and effective *in vitro* teratoma surrogate assay.

Population heterogeneity arising from microenvironmental differences applies broadly to adherent populations and is increasingly recognized as a major obfuscating factor in drug screening campaigns[40]. We believe the methods presented herein are broadly applicable to adherent cell types. We have developed 96μCP based assays for mouse epiblast stem cells, and hPSC-derived cardiac and endoderm cells with minimal modification to the base media, substrate, and pattern size. Applying these concepts towards rapid characterization of the signaling involved in cell fate decisions of differentiated cell types is a promising strategy to accelerate the drive towards clinical regenerative medicine and drug screening of hPSC disease models.

Methods

Cell culture

HESC lines H9, H1 and H7 were obtained from the WiCell Research Institute. ZAN3 and ZAN11 were derived from activated CD3+ T cells enriched from umbilical cord blood (see below). HES2 (hESC) was provided by G. Keller (McEwen Centre for Regenerative Medicine/University Health Network). BJ1D (hiPSC) was provided by M. Radisic (University of Toronto). 110 (hiPSC)[41] and CA1 (hESC)[42] were provided by A. Nagy (Samuel Lunenfeld Research Institute). PDX1 (MEL1-derived PDX1-GFP hESC) was provided by D. Melton (Harvard University). Runx1 (HES3-derived Runx1-GFP hESC) was provided by A. Elefanty (Monash University). R306C[43], RTT-Δ3-4 #37, and T158M #5 (ref. 44), all Rett syndrome hiPSC disease models, as well as BJ4YA (hiPSC) were provided by J. Ellis (The Hospital for Sick Children). H9, H1, H7, ZAN3, ZAN11, and PDX1 cells were routinely cultured on feeder layers of irradiated MEFs feeders in knockout (KO)-Dulbecco's modified Eagle's medium (DMEM) (Invitrogen) with 20 % KO-serum replacement (Invitrogen) (KO-DMEM) and supplemented with 4 ng mL^{-1} FGF-2 (PeproTech). Cells were passaged 1:4–1:6 every 4–5 days, and were disassociated into small clumps using 0.1 % collagenase IV (Invitrogen). HES2 and Runx1 were cultured on growth factor reduced Matrigel (MG) in KO-DMEM supplemented with 20 ng mL^{-1} FGF-2 (PeproTech), and were passaged every 4–5 days using TrypLE Express (Invitrogen). CA1 was cultured on MG using NutriStem (Stemgent) as per manufacturer's instructions. BJ1D, 110, R306C, RTT-Δ3-4 #37, T158M #5, and BJ4YA were cultured on MG using mTeSR1 (STEMCELL Technologies) as per manufacturer's instructions. All cell line stocks were confirmed negative for mycoplasma contamination.

Microcontact printing of substrate into 96-well plates

PDMS stamps were fabricated using standard soft lithography techniques[45], with the exception that liquid PDMS was cast into a Teflon mould before curing, allowing control of the shape of the PDMS stamp. PDMS stamps were cast consisting of rectangular base with 24 posts (6 × 4) with micropatterned surfaces configured to enable microcontact printing directly into 96-well plates. The microcontact printing follows a protocol employed previously[46]. Substrate solution consisted of either MG diluted 1:30 in phosphate buffered saline (PBS), or a solution of 0.00125 % fibronectin (Sigma-Aldrich, F1141) and 0.002 % gelatin (Sigma-Aldrich, G9391). Substrate solution was deposited onto the patterned surface of ethanol sterilized PDMS stamps for 4h at room temperature. Stamps were rinsed with ddH2O, dried gently with N2 gas, and placed into tissue-culture treated 96-well plates (Costar). Stamps were incubated in the 96-well plates for 7–10 min in a humidity chamber (Relative humidity 55–70 %). The stamps were then removed and substrates were passivated with 5 % weight Pluronic F-127 (Sigma-Aldrich) in ddH20 for 1 h.

Seeding hiPSCs onto patterned substrates

hiPSCs were dissociated using TrypLE™ for three min. TrypLE™ was inactivated by adding media containing 20 % KO-serum replacement (SR) (Invitrogen). Cells were centrifuged and resuspended in either XVIVO10™ (XV) or SF media both supplemented with 40 ng mL^{-1} bFGF (R&D), 10 ng mL^{-1} activin A (R&D), 10 μM ROCK inhibitor Y-27632 (Tocris)

and 7 μg mL^{-1} additional insulin. SF media is a modification of DC-HAIF[47] and consists of DMEM/F12, 1x Nonessential amino acids, 50 U mL^{-1} Penicillin, 50 μg mL^{-1} Streptomycin, 10 μg mL^{-1} bovine Transferrin, 0.1 mM β-Mercaptoethanol (all Invitrogen), 2 % fatty acid-free Cohn's fraction V BSA (Serologicals), 1x Trace Elements A, B & C (Mediatech), 50 μg mL^{-1} Ascorbic Acid (Sigma) and 7 μg mL^{-1} recombinant human insulin. XV includes XVIVO10™ (Lonza) supplemented with 2 mM L-Glutamine, 0.1 mM β-Mercaptoethanol and 1x Nonessential amino acids. Cells were seeded at 10^5 cells per well (or as described in text) and incubated. After 6 h, cells were washed with PBS two times and incubated a further 42 h with fresh media as indicated (SF supplemented with factors, or MEF-CM).

Immunocytochemistry and image analysis

Plates were fixed for 30 min in 3.7 % formaldehyde and permeabilized for 3 min in 100 % methanol. Plates were imaged and quantitatively analyzed using the Cellomics Arrayscan VTI platform and Target Activation algorithm (Thermo Scientific). This algorithm generates nuclear masks, provides single cell nuclear intensity values for protein expression (Oct4, Sox2 etc.), DNA content through DAPI staining, as well as spatial x- and y-coordinates of the nuclei centroids. Insufficiently patterned wells were excluded from analysis based on a predetermined number of cells per well. To aid in pattern visualization and quality control, we developed a publically available MATLAB script to plot these x- and y-coordinates for all wells in a 96-well plate (Nazareth, E. Analysis and visualization of Cellomics data. MATLAB Central File Exchange, http://www.mathworks.com/matlabcentral/fileexchange/43107). Clustering of cells into colonies using Euclidean distance was performed using clusterData (Shoelson, B. clusterData. MATLAB Central File Exchange, http://www.mathworks.com/matlabcentral/fileexchange/35014-clusterdata). Fluorescent images were obtained of Oct4 (1:500; BD), Sox2 (1:500 R&D Systems), Nanog (1:500; Cell Signaling), Tra-1-60 (1:500 R&D Systems), Brachyury (1:200; R&D Systems), Snail (1:200; R&D Systems), and GATA4 (1:200; R&D Systems). Primary antibodies were incubated overnight in 10 % FBS in PBS at 4° C. AlexaFluor secondary antibodies (1:500; Molecular Probes) were incubated for 1 h in 10% FBS in PBS at room temperature. 16 bit TIFF images were obtained for each channel, contrast adjustment was performed identically across all controls, and channels were combined into pseudo-colored composite images.

hiPSC derivation

Umbilical cord blood samples were collected from consenting donors according to ethically approved procedures at Mt. Sinai Hospital (Toronto, ON, Canada). Activated $CD3^+$ T cells enriched from umbilical cord blood were reprogrammed as described previously[48]. T cells were enriched from umbilical cord blood using an EasySep human T cell enrichment kit (StemCell Technologies; cat# 19051). They were expanded for four days using Dynabeads human T-activator CD3/CD28 beads (Invitrogen; cat# 111-61D) and 30U per mL recombinant human IL-2 (R&D; cat# 202-IL-010) in OpTmizer T cell expansion serum-free media (Invitrogen; cat#A1048501). Mutant Sendai virus encoding human Oct4, Sox2, KLF4 and c-MYC (kindly provided by DNAVEC Corporation) were added to the cells at MOI 20 on day five. T cell media was replenished on day six and the cells were plated onto irradiated MEF feeders on day seven in hPSC medium with 5 ng mL^{-1} bFGF. Media was exchanged every two days until hiPSC colonies were picked and characterized three weeks later.

hiPSC cardiomyogenic and endoderm induction

hiPSC cardiomyogenic induction was performed using a serum-free, aggregate-based strategy described elsewhere[49]. A single cell suspension of hiPSC was centrifuged into 400 μm-sized AggreWell™ inserts (Stemcell Technologies) at a density of 500 cells per microwell and cells were allowed to aggregate over night. On day one, mesoderm formation was induced using 5 ng mL^{-1} bFGF and varying concentrations of Activin A as indicated. On day four, cells were transferred to LowCluster plates (Nunc) and further differentiation towards the cardiac lineage was induced with 10 ng mL^{-1} VEGF and 150 ng mL^{-1} DKK1 for four days. Subsequently, cells were maintained in 10 ng mL^{-1} VEGF and 5 ng mL^{-1} bFGF. Custom defined media provided in kind by G. Keller was used as the base media. Cells were kept under hypoxic conditions (5 % O_2) from day 0–12 and then transferred to normoxic conditions. Endoderm induction into $PDX1^+$ pancreatic progenitor cells was performed as described by Nostro et. al[50]. Endoderm induction into $Foxa2^+Sox17^+$ definitive endoderm was performed as described by Rezania et. al[51] in 96-well plates.

Flow cytometry

HiPSC-derived cardiomyocyte aggregates were incubated in collagenase type II (1 mg mL^{-1}; Worthington, LS004176) in Hank's Balanced Salt Solution over night at room temperature and pipetted vigorously to obtain a single cell suspension which was then fixed in 4 % paraformaldehyde over night at 4° C. Cells were permeabilized using IntraPrep™ Permeabilization Reagent (Immunotech, A07803). Cardiac Troponin T primary antibody (Thermo Scientific, MS-295-P) was used at 1:200 and AlexaFluor 647 donkey anti-mouse IgG secondary antibody (Molecular Probes, A31571) at 1:200. Cells were analyzed using a FACSCanto (BD Biosciences) flow cytometer.

Estimation of endogenous pathway activation

To estimate endogenous pathway activation we obtained the cell fate response to the pathway agonist and antagonist, both at saturating levels as determined by dose-curves. The baseline response (in SF basal media alone) can then be calibrated within this range using the following equation:

$$\%Dynamic\ Range = \frac{X_{SF\ Ctrl} - X_{Antagonist}}{X_{Agonist} - X_{Antagonist}} \quad \text{Eqn. 1}$$

Statistical analysis

Statistics were computed using one way analysis of variance (ANOVA), two-factor ANOVA, or linear regression as indicated. Error bars on plots represent standard deviation (s.d.) of three or more replicate wells except where indicated differently. All statistics were computed in MATLAB using p-values as indicated. Hierarchical clustering was performed with MeV (MultiExperiment Viewer, http://www.tm4.org/mev/) using euclidan distance as the similarity metric (centered) and centroid linkage as the clustering method.

Supplementary Material

Refer to Web version on PubMed Central for supplementary material.

Acknowledgments

This work is funded by the Canadian Institutes of Health Research (CIHR) (P.W.Z). E.J.P.N. is supported by a CIHR Frederick Banting and Charles Best Canada Graduate Scholarships Doctoral Award. P.B.L. is supported by a Heart & Stroke Richard Lewar Centre of Excellence Studentship award. S.S. is supported by a Vanier Canada Graduate Scholarship. P.W.Z. is supported as the Canada Research Chair in Stem Cell Bioengineering. We thank S. Foster for illustrating Supplementary Fig. 1. Ligands provided in kind by the International Stem Cell Initiative. We thank G. Keller (McEwen Centre for Regenerative Medicine/University Health Network), M. Radisic (University of Toronto), A. Nagy (Samuel Lunenfeld Research Institute), D. Melton (Harvard University), A. Elefanty (Monash University), and J. Ellis (The Hospital for Sick Children) for provision of cell lines. We thank Peter Andrews and Martin Pera for helpful discussion.

References

1. Levenstein ME, et al. Basic fibroblast growth factor support of human embryonic stem cell self-renewal. Stem Cells. 2006; 24:568–574. [PubMed: 16282444]
2. Bendall SC, et al. IGF and FGF cooperatively establish the regulatory stem cell niche of pluripotent human cells in vitro. Nature. 2007
3. Vallier L, Alexander M, Pedersen RA. Activin/Nodal and FGF pathways cooperate to maintain pluripotency of human embryonic stem cells. J Cell Sci. 2005; 118:4495–4509. [PubMed: 16179608]
4. Avery S, Zafarana G, Gokhale PJ, Andrews PW. The role of SMAD4 in human embryonic stem cell self-renewal and stem cell fate. Stem Cells. 2010; 28:863–873. [PubMed: 20235236]
5. Amit M, et al. Dynamic suspension culture for scalable expansion of undifferentiated human pluripotent stem cells. Nat Protoc. 2011; 6:572–579. [PubMed: 21527915]
6. Daheron L, et al. LIF/STAT3 signaling fails to maintain self-renewal of human embryonic stem cells. Stem Cells. 2004; 22:770–778. [PubMed: 15342941]
7. Sato N, Meijer L, Skaltsounis L, Greengard P, Brivanlou AH. Maintenance of pluripotency in human and mouse embryonic stem cells through activation of Wnt signaling by a pharmacological GSK-3-specific inhibitor. Nature medicine. 2004; 10:55–63.
8. Dravid G, et al. Defining the role of Wnt/beta-catenin signaling in the survival, proliferation, and self-renewal of human embryonic stem cells. Stem Cells. 2005; 23:1489–1501. [PubMed: 16002782]
9. Akopian V, et al. Comparison of defined culture systems for feeder cell free propagation of human embryonic stem cells. In vitro cellular & developmental biology. 2010
10. Peerani R, et al. Niche-mediated control of human embryonic stem cell self-renewal and differentiation. Embo J. 2007; 26:4744–4755. [PubMed: 17948051]
11. McBeath R, Pirone DM, Nelson CM, Bhadriraju K, Chen CS. Cell shape, cytoskeletal tension, and RhoA regulate stem cell lineage commitment. Dev Cell. 2004; 6:483–495. [PubMed: 15068789]
12. Maherali N, Hochedlinger K. Guidelines and techniques for the generation of induced pluripotent stem cells. Cell Stem Cell. 2008; 3:595–605. [PubMed: 19041776]
13. Chambers SM, et al. Highly efficient neural conversion of human ES and iPS cells by dual inhibition of SMAD signaling. Nature biotechnology. 2009
14. Cai J, et al. Generation of homogeneous PDX1(+) pancreatic progenitors from human ES cell-derived endoderm cells. Journal of molecular cell biology. 2009; 2:50–60. [PubMed: 19910415]
15. Hwang YS, et al. Microwell-mediated control of embryoid body size regulates embryonic stem cell fate via differential expression of WNT5a and WNT11. Proc Natl Acad Sci U S A. 2009; 106:16978–16983. [PubMed: 19805103]
16. Sun N, et al. Patient-specific induced pluripotent stem cells as a model for familial dilated cardiomyopathy. Sci Transl Med. 2012; 4:130ra147.

17. Yu PB, et al. BMP type I receptor inhibition reduces heterotopic ossification. Nature medicine. 2008; 14:1363–1369.
18. Xu C, et al. Feeder-free growth of undifferentiated human embryonic stem cells. Nature biotechnology. 2001; 19:971–974.
19. Wang L, et al. Self-renewal of human embryonic stem cells requires insulin-like growth factor-1 receptor and ERBB2 receptor signaling. Blood. 2007
20. Xu RH, et al. BMP4 initiates human embryonic stem cell differentiation to trophoblast. Nature biotechnology. 2002; 20:1261–1264.
21. Pera MF, et al. Regulation of human embryonic stem cell differentiation by BMP-2 and its antagonist noggin. J Cell Sci. 2004; 117:1269–1280. [PubMed: 14996946]
22. Vallier L, et al. Early cell fate decisions of human embryonic stem cells and mouse epiblast stem cells are controlled by the same signalling pathways. PLoS One. 2009; 4:e6082. [PubMed: 19564924]
23. Smith JR, et al. Inhibition of Activin/Nodal signaling promotes specification of human embryonic stem cells into neuroectoderm. Dev Biol. 2008; 313:107–117. [PubMed: 18022151]
24. Vallier L, Reynolds D, Pedersen RA. Nodal inhibits differentiation of human embryonic stem cells along the neuroectodermal default pathway. Dev Biol. 2004; 275:403–421. [PubMed: 15501227]
25. Paige SL, et al. Endogenous Wnt/beta-catenin signaling is required for cardiac differentiation in human embryonic stem cells. PLoS One. 2010; 5:e11134. [PubMed: 20559569]
26. Vallier L, et al. Activin/Nodal signalling maintains pluripotency by controlling Nanog expression. Development. 2009
27. Lowell S, Benchoua A, Heavey B, Smith AG. Notch promotes neural lineage entry by pluripotent embryonic stem cells. PLoS Biol. 2006; 4:e121. [PubMed: 16594731]
28. Boyer LA, et al. Core transcriptional regulatory circuitry in human embryonic stem cells. Cell. 2005; 122:947–956. [PubMed: 16153702]
29. Mossman AK, Sourris K, Ng E, Stanley EG, Elefanty AG. Mixl1 and oct4 proteins are transiently co-expressed in differentiating mouse and human embryonic stem cells. Stem Cells Dev. 2005; 14:656–663. [PubMed: 16433620]
30. Chng Z, Teo A, Pedersen RA, Vallier L. SIP1 mediates cell-fate decisions between neuroectoderm and mesendoderm in human pluripotent stem cells. Cell Stem Cell. 2010; 6:59–70. [PubMed: 20074535]
31. James D, Levine AJ, Besser D, Hemmati-Brivanlou A. TGFbeta/activin/nodal signaling is necessary for the maintenance of pluripotency in human embryonic stem cells. Development. 2005; 132:1273–1282. [PubMed: 15703277]
32. Wang G, et al. Noggin and bFGF cooperate to maintain the pluripotency of human embryonic stem cells in the absence of feeder layers. Biochem Biophys Res Commun. 2005; 330:934–942. [PubMed: 15809086]
33. Gonzalez R, et al. Screening the mammalian extracellular proteome for regulators of embryonic human stem cell pluripotency. Proc Natl Acad Sci U S A. 2010; 107:3552–3557. [PubMed: 20133595]
34. Greber B, et al. Conserved and divergent roles of FGF signaling in mouse epiblast stem cells and human embryonic stem cells. Cell Stem Cell. 2010; 6:215–226. [PubMed: 20207225]
35. Vallier L, et al. Signaling pathways controlling pluripotency and early cell fate decisions of human induced pluripotent stem cells. Stem Cells. 2009; 27:2655–2666. [PubMed: 19688839]
36. Nostro MC, et al. Stage-specific signaling through TGFbeta family members and WNT regulates patterning and pancreatic specification of human pluripotent stem cells. Development. 2011; 138:861–871. [PubMed: 21270052]
37. Osafune K, et al. Marked differences in differentiation propensity among human embryonic stem cell lines. Nature biotechnology. 2008; 26:313–315.
38. Yang L, et al. Human cardiovascular progenitor cells develop from a KDR+ embryonic-stem-cell-derived population. Nature. 2008; 453:524–528. [PubMed: 18432194]

39. Kattman SJ, et al. Stage-specific optimization of activin/nodal and BMP signaling promotes cardiac differentiation of mouse and human pluripotent stem cell lines. Cell Stem Cell. 2011; 8:228–240. [PubMed: 21295278]
40. Snijder B, et al. Population context determines cell-to-cell variability in endocytosis and virus infection. Nature. 2009; 461:520–523. [PubMed: 19710653]
41. Hussein SM, et al. Copy number variation and selection during reprogramming to pluripotency. Nature. 2011; 471:58–62. [PubMed: 21368824]
42. Amps K, et al. Screening ethnically diverse human embryonic stem cells identifies a chromosome 20 minimal amplicon conferring growth advantage. Nature biotechnology. 2011; 29:1132–1144.
43. Hotta A, et al. Isolation of human iPS cells using EOS lentiviral vectors to select for pluripotency. Nat Methods. 2009; 6:370–376. [PubMed: 19404254]
44. Cheung AY, et al. Isolation of MECP2-null Rett Syndrome patient hiPS cells and isogenic controls through X-chromosome inactivation. Hum Mol Genet. 2011; 20:2103–2115. [PubMed: 21372149]
45. Peerani R, Bauwens C, Kumacheva E, Zandstra PW. Patterning mouse and human embryonic stem cells using micro-contact printing. Methods Mol Biol. 2009; 482:21–33. [PubMed: 19089347]
46. Tan JL, Liu W, Nelson CM, Raghavan S, Chen CS. Simple approach to micropattern cells on common culture substrates by tuning substrate wettability. Tissue Eng. 2004; 10:865–872. [PubMed: 15265304]
47. Wang L, et al. Self-renewal of human embryonic stem cells requires insulin-like growth factor-1 receptor and ERBB2 receptor signaling. Blood. 2007
48. Seki T, Yuasa S, Fukuda K. Generation of induced pluripotent stem cells from a small amount of human peripheral blood using a combination of activated T cells and Sendai virus. Nat Protoc. 2012; 7:718–728. [PubMed: 22422317]
49. Bauwens CL, et al. Geometric control of cardiomyogenic induction in human pluripotent stem cells. Tissue Eng Part A. 2011; 17:1901–1909. [PubMed: 21417693]
50. Nostro MC, et al. Stage-specific signaling through TGFbeta family members and WNT regulates patterning and pancreatic specification of human pluripotent stem cells. Development. 2011; 138:861–871. [PubMed: 21270052]
51. Rezania A, et al. Maturation of human embryonic stem cell-derived pancreatic progenitors into functional islets capable of treating pre-existing diabetes in mice. Diabetes. 2012; 61:2016–2029. [PubMed: 22740171]

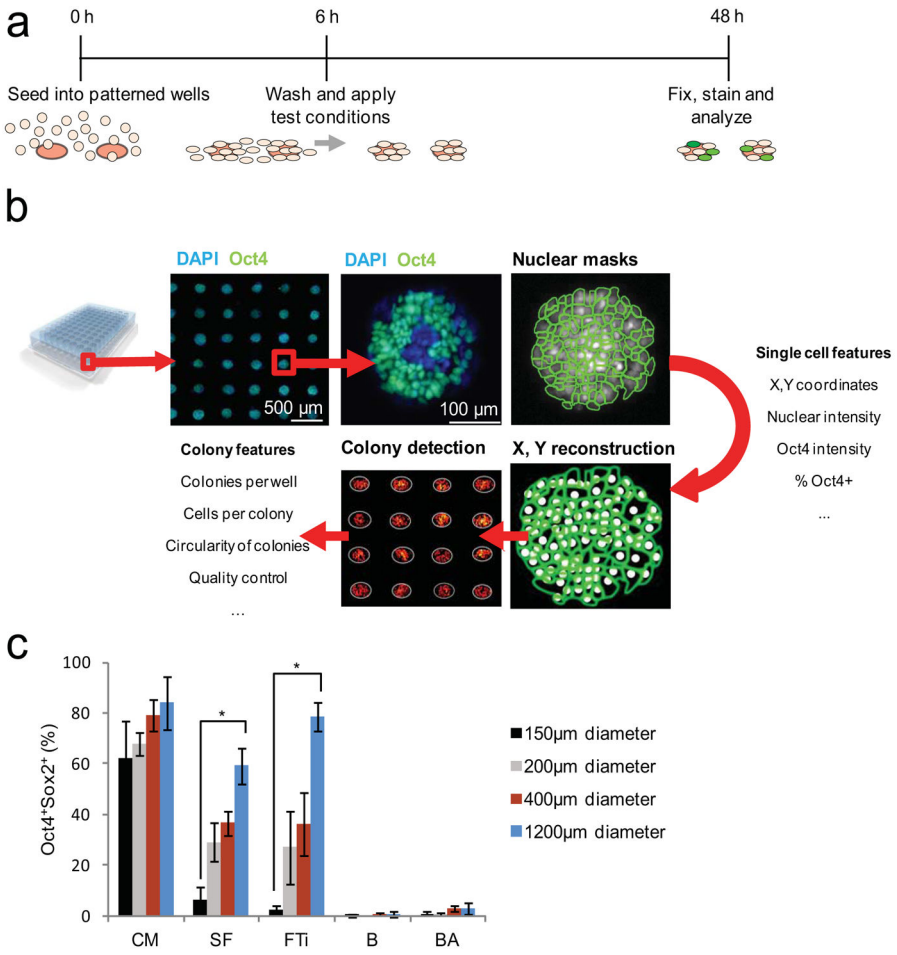

Fig. 1. Optimization of the 96µCP platform

(**a**) Schematic of the assay design. Cell substrates are first patterned into standard 96-well plates using micro-contact printing. A single cell suspension of the population of interest is then generated and seeded onto the 96-well plates. The plates are then incubated for 6 h, allowing the cells to settle and adhere to the patterned substrates. Plates are then washed two times with PBS and test media (i.e. base media with factors) is added to each well. Plates are fixed 48 h after seeding and subsequently stained. (**b**) Sample image of a patterned hPSC colony viewed at 20x, and 25 stitched fields showing an array of colonies at the bottom of a well in a 96-well plate. DAPI staining is used to obtain nuclear masks which enable single cell analysis. The single cell features can be used to reconstruct vectorized figures of the wells. Using the x- and y-coordinates, cells can be clustered into colonies to enable colony-level analysis. (**c**) Colony size optimization. FnGel was patterned in different diameter islands as indicated. Cells were patterned and the response to murine embryonic fibroblast conditioned media (CM), base media alone (SF), SF with FGF2 and SB431542 (FTi), SF with BMP4 (B), or SF with BMP4 and activin A (BA) was tested. * ANOVA $p < 0.01$ and Tukey post-hoc $p < 0.01$. Error bars, s.d. (n = 3).

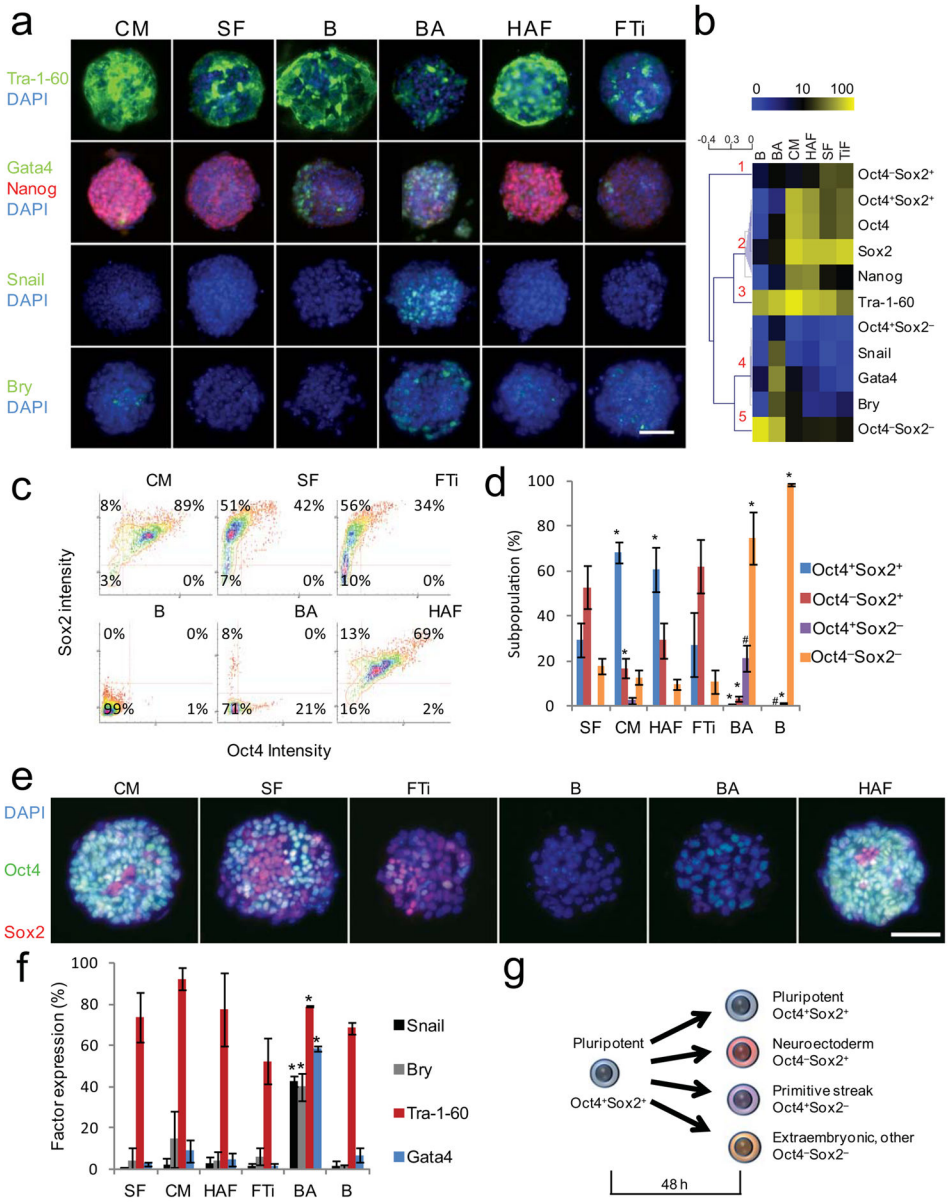

Fig. 2. Single cell protein profiling reveals Oct4 and Sox2 mark early cell fates

(**a**) Sample images of control conditions stained for Tra-1-60, Gata4, Nanog, Snail, and Brachyury (Bry). Scale bar 100 μm. (**b**) 2D hierarchical clustering of protein expression levels (%positive) of markers and sets of markers across control conditions. Left panel displays sample similarity tree, with samples clustered using a distance threshold of 0.4. Clusters are indicated in red numerals. (**c**) Sample plots of Oct4 and Sox2 intensity values from controls. Thresholds can be based on these controls to classify cells as positive or negative for each marker. (**d**) Quantification of Oct4 and Sox2 subpopulations in control conditions. Statistically compared to SF control value, * ANOVA $p < 0.01$ and Tukey post-hoc $p < 0.01$, # ANOVA $p < 0.005$ and Tukey post-hoc $p < 0.05$. Error bars, s.d. (n = 3). (**e**) Sample composite images showing DAPI (blue), Oct4 (green), and Sox2 (red) expression in controls. Scale bar 100 μm. (**f**) Quantification of Snail, Bry, Tra-1-60, and Gata4 expression

in control conditions. * Statistically compared to SF control value, ANOVA $p < 0.01$ and Tukey post-hoc $p < 0.01$. Error bars, s.d. ($n = 3$). (**g**) Summary of Oct4 and Sox2 subpopulations.

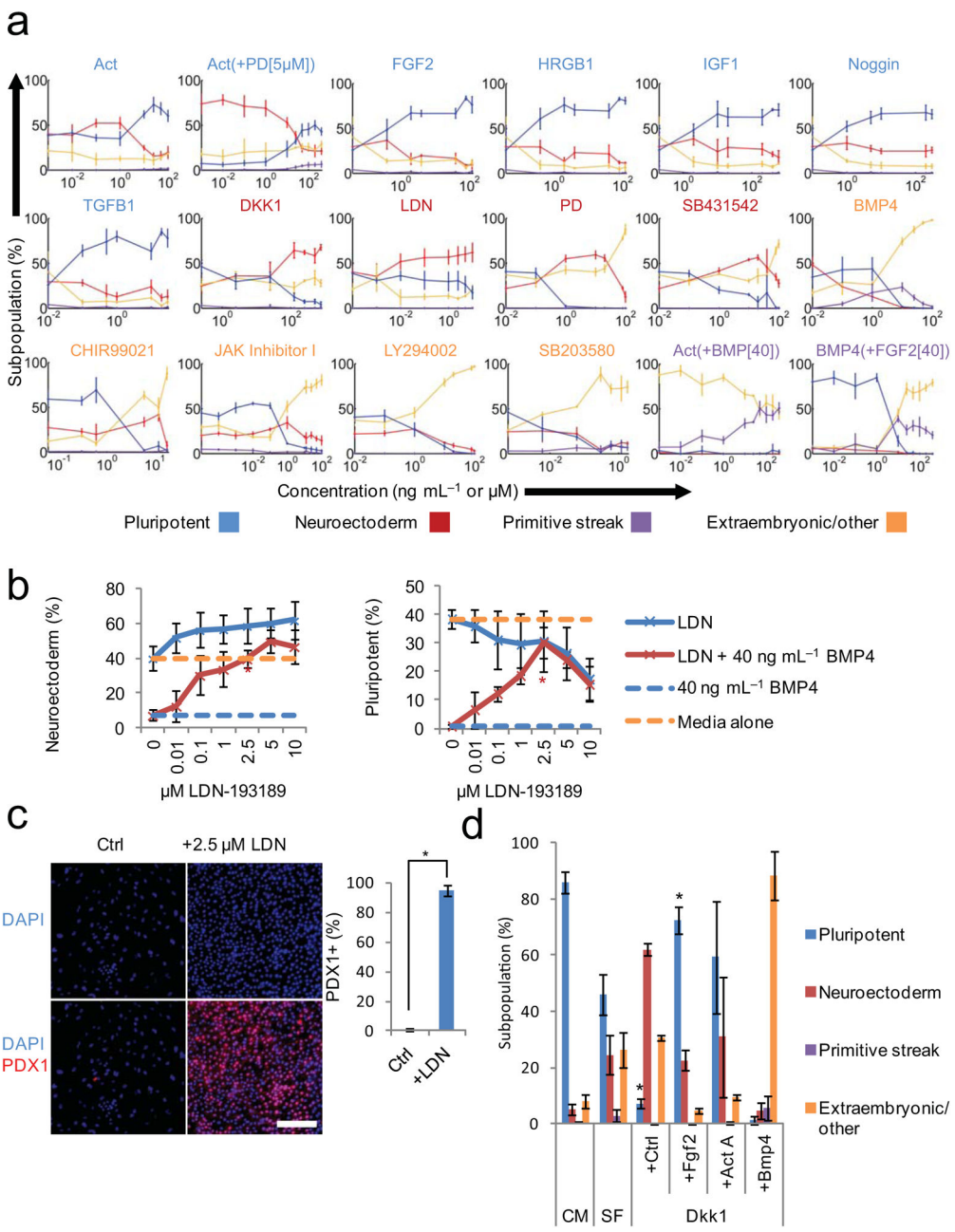

Fig. 3. Characterization of factors modulating pluripotency, neuroectoderm, primitive streak, and extraembryonic cell fate choices

(**a**) Dose curves of development signaling factors. Title color indicates predominant effect of each factor: promoting pluripotency (blue), neuroectoderm (red), extraembryonic (green), or primitive streak (purple), or a mixed effect (orange). Ligand concentration is shown in ng/mL, small molecule concentration is shown in μM. Error bars, s.d. (n > 2). (**b**) Dose curve of Alk2/3/6 inhibitor LDN-193189 with and without 40ng/mL BMP4. Baseline pluripotency and neuroectoderm conditions in SF media alone or SF with BMP4 are shown with dotted lines. Statistically compared to "0" control values, * ANOVA $p < 0.01$ and Tukey post-hoc $p < 0.01$. Error bars, s.d. (n = 3). (**c**) LDN addition during stage two of

endoderm differentiation enables generation of PDX1+ endoderm cells. Scale bar 100 μm. *ANOVA $p < 0.0001$. Error bars, s.d. (n = 3). (**d**) DKK1 inhibits pluripotency and promotes neuroectoderm, but this effect is masked by FGF2, activin A or BMP. * ANOVA $p < 0.01$ and Tukey post-hoc $p < 0.01$. Error bars, s.d. (n = 3).

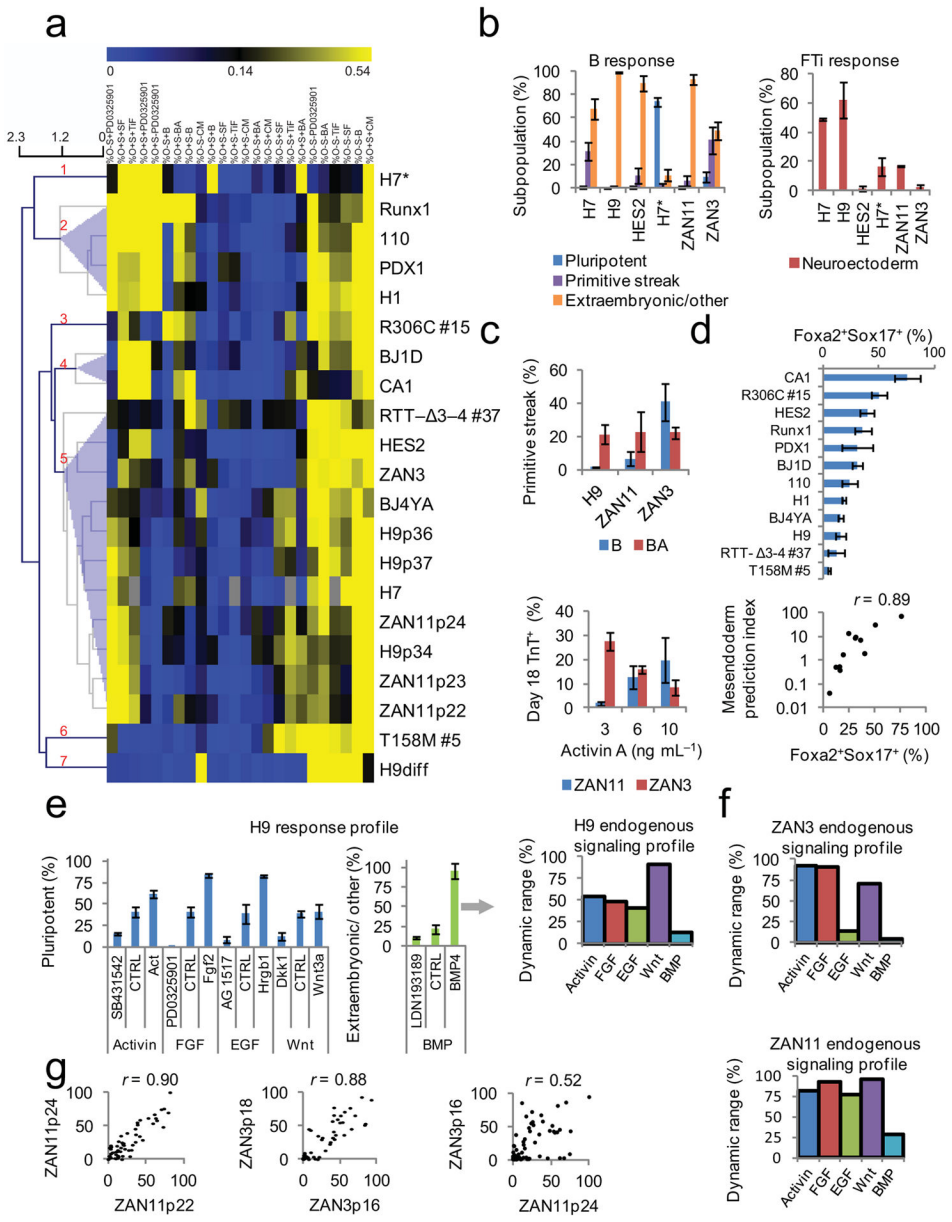

Fig. 4. Quantitative assessment of cell line specific endogenous signaling and germ layer differentiation efficiency

(**a**) Hierarchical clustering of cell line responses to controls (Euclidean distance similarity metric, average linkage clustering). Left panel displays sample similarity tree, with samples clustered using a distance threshold of 1.4. Clusters are indicated in red numerals. (**b**) Germ layer differentiation of multiple cell lines can be compared on-chip in a rapid, controlled, and quantitative manner. Error bars, s.d. (n = 3). (**c**) i) Activin A has differential effects on day 2 primitive streak induction in ZAN3 and ZAN11 cell lines. * ANOVA, $p < 0.005$. Error bars, s.d. (n = 3) ii) At day 18 of cardiac induction, activin A has differential effects on cardiac Troponin T (TnT) expression in ZAN3 and ZAN11 cell lines ($p < 0.005$, Two-Factor ANOVA with n = 2, independent passages), with Activin A increasing primitive streak in ZAN11s and decreasing primitive streak in ZAN3s (both >95 percent confidence using

linear regression). Error bars, s.d. (n = 2). (**d**) i) Definitive endoderm induction efficiencies of 12 cell lines. Error bars, s.d. (n = 2). ii) Correlation of cell line Mesendoderm prediction index values from day 2 to actual definitive endoderm induction efficiencies at day 5 for a panel of cell lines ($r = 0.89$, $p < 0.0001$). (**e**) i) The response of H9s to signaling pathway agonists and antagonists. Error bars, s.d. (n = 3). ii) Estimated endogenous signaling levels of specific pathways for H9 (Eqn. 1, **Methods**). iii) Estimated endogenous signaling levels for ZAN3 and ZAN11 cell lines. iv) Passage to passage correlation of endogenous signaling profiles. The 60 response outputs (4 readouts × 15 conditions) were obtained for multiple passages for ZAN11 and ZAN3 showing high passage-to-passage correlation (ZAN 11 $r = 0.90$, ZAN3 $r = 0.88$). Comparison of ZAN3 and ZAN11 shows low line-to-line correlation ($r = 0.52$).

Table 1

Factor Characterization

Promotes	Factor	Recommended Concentration
Pluripotency	Activin A	10 ng/mL (0.8 nM)
	FGF2 (Fibroblast growth factor 2)	80 ng/mL (5 nM)
	HRGβ1 (Heregulin-β1)	80 ng/mL (10.6 nM)
	IGF1 (Insulin-like growth factor 1)	10 ng/mL (1.3 nM)
	LDN-193189 (“LDN”, ALK2/3/6 inhibitor)	2.5 μM
	Noggin	10 ng/mL (0.4 nM)
	TGFβ1 (Transforming growth factor- β1)	1 ng/mL (0.08 nM)
Neuroectoderm	DKK1 (Dickkopf Homolog 1 Protein)	125 ng/mL (3.1 nM)
	LDN-193189 (“LDN”, ALK2/3/6 inhibitor)	2.5 μM
	PD0325901 (“PD”, MEK inhibitor)	1 μM
	SB431542 (ALK4/5/7 inhibitor)	10 μM
Primitive Streak	Activin A	10–100 ng/mL (0.8 – 8 nM)
	BMP4 (Bone morphogenetic protein 4)	10–100 ng/mL (0.8 – 8 nM)
Extraembryonic/Other	BMP4 (Bone morphogenetic protein 4)	40 ng/mL (3.2 nM)
	CHIR99021 (GSK3β inhibitor)	6 μM
	JAK Inhibitor I (JAK1/2/3 inhibitor)	10 μM
	LY294002 (PI3K inhibitor)	10 μM
	SB203580 (p38 MAPK inhibitor)	0.3 μM
No Observed Action [Range Tested]	BAFF (B-cell activating factor) [0.1–100 ng/mL]	
	Betacellulin [0.1–100 ng/mL]	
	FGF4 (Fibroblast growth factor 4) [0.1–100 ng/mL]	
	FLT3L (FMS-like tyrosine kinase 3 ligand) [0.1–100 ng/mL]	
	GDF3 (Growth differentiation factor-3) [0.1–200 ng/mL]	
	LIF (human Leukemia inhibitory factor) [0.0001–200 ng/mL]	
	PDGF (platelet-derived growth factor-AB) [0.01–100ng/mL]	
	SCF (Stem cell factor) [0.01–100 ng/mL]	
	VEGF (Vascular endothelial growth factor) [0.01–100ng/mL]	
	Wnt3a [0.01–100ng/mL]	
	Wnt5a [0.1–200 ng/mL]	
	Y27632 (“ROCKi”, ROCK inhibitor) [0.1–100 μM]	